Magnetic Moment of the Proton in Units of the Bohr Magneton; the Magnetic Moment of the Electron*

SIDNEY LIEBES, JR.,† AND PETER FRANKEN‡
Department of Physics, Stanford University, Stanford, California
(Received May 27, 1959)

The details of a previously reported measurement of the proton magnetic moment in units of the Bohr magneton are given. This ratio of moments, which is obtained from common magnetic field observations of the nuclear magnetic resonance frequency of protons in a spherical sample of mineral oil and the cyclotron frequency of free low-energy electrons, is found to be $\mu_{p(\text{oil})}/\mu_0=(657.462\pm0.003)^{-1}$, where the uncertainty represents the estimated 50% probable error. The magnetic moment of the free proton is found, upon application of the appropriate diamagnetic correction factor, to be $\mu_p/\mu_0=(657.442\pm0.003)^{-1}$. The present result may be combined with reported values for the ratio of the magnetic moment of the electron to the moment of the proton to yield for the magnetic moment of the free electron in units of the Bohr magneton,

$$\mu_e/\mu_0=1.001168\pm0.000005$$
$$=1+(\alpha/2\pi)+(1.2\pm0.9)(\alpha^2/\pi^2),$$

where the uncertainty is the estimated 50% probable error. This result is to be compared with the current theoretically estimated value for this quantity,

$$\mu_e/\mu_0=1+(\alpha/2\pi)-0.328(\alpha^2/\pi^2)$$
$$=1.0011596.$$

1. INTRODUCTION

WE wish to present the details and final results of a previously reported measurement[1] of the magnetic moment of the proton μ_p in units of the Bohr magneton $\mu_0=e\hbar/2mc$. This result is used in a determination of the magnetic moment of the electron in units of the Bohr magneton μ_e/μ_0.

One of the striking achievements of the present formulation of quantum electrodynamics has been the evaluation of radiative correction terms to the Dirac value for the magnetic moment of the free electron. These terms provide one of the few opportunities for comparison of a quantitative prediction of quantum electrodynamics with experiment. Currently, the most precise experimental value of the electron moment in Bohr magnetons μ_e/μ_0 is obtained by combining the result of an experiment of the present type μ_p/μ_0 with a determination of μ_e/μ_p. At the time the present work was undertaken the precision of the comparison between theory and experiment was limited primarily by the uncertainty associated with the available experimental value for μ_p/μ_0.[2]

The quantity μ_p/μ_0 also can be combined with other experimental data to establish values for such physical constants as Avagadro's number, Planck's constant, the fine structure constant, the charge of the electron, the electron-proton mass ratio, the Bohr magneton, and the absolute magnetic moment of the proton.[3]

2. THEORETICAL AND EXPERIMENTAL STATUS OF THE MAGNETIC MOMENT OF THE ELECTRON

The quantum electrodynamical radiative correction terms to the magnetic moment of the electron are expressed in powers of the fine structure constant $\alpha=e^2/\hbar c$. The term of order α was first calculated by Schwinger.[4] The term of order α^2 was originally computed by Karplus and Kroll[5] and has been recently re-evaluated by Petermann[6] and by Sommerfield.[7] The current theoretical estimate for the free electron moment is[6,7]

$$\mu_e/\mu_0=1+(\alpha/2\pi)-0.328(\alpha^2/\pi^2)$$
$$=1.0011596, \qquad (2.1)$$

where the fine structure constant has been assigned the value[3] $\alpha^{-1}=137.0391\pm0.0006$.

The only measurement of μ_p/μ_0 published prior to the performance of the present experiment was that of Gardner and Purcell[2]; the stated limit of error was 12 ppm (parts per million). Four independent measure-

* This work was supported by a grant from Research Corporation, by the Office of Naval Research, and by the U. S. Atomic Energy Commission. This report is based on a dissertation submitted to the Department of Physics and the Committee on Graduate Study at Stanford University in partial fulfillment of the requirements for the degree of Doctor of Philosophy by Sidney Liebes, Jr., November, 1957.

† Present address: Palmer Physical Laboratory, Princeton University, Princeton, New Jersey.

‡ Present address: The Harrison M. Randall Laboratory of Physics, University of Michigan, Ann Arbor, Michigan.

[1] P. Franken and S. Liebes, Jr., Phys. Rev. **104**, 1197 (1956); see also S. Liebes, Jr., Ph.D. thesis (unpublished).

[2] J. H. Gardner and E. M. Purcell, Phys. Rev. **76**, 1262 (1949); J. H. Gardner, Phys. Rev. **83**, 996 (1951). A modification of this experiment was undertaken by R. W. Nelson, Ph.D. thesis, Harvard University, 1953 (unpublished).

[3] See, for example, E. R. Cohen and J. W. M. DuMond, in *Encyclopedia of Physics*, edited by S. Flügge (Springer-Verlag, Berlin, 1957), Vol. 35, pp. 1 ff.; Cohen, DuMond, Layton, and Rollett, Revs. Modern Phys. **27**, 363 (1955); E. R. Cohen and J. W. M. DuMond, Phys. Rev. Letters **1**, 291 (1958).

[4] J. Schwinger, Phys. Rev. **73**, 416 (1948).

[5] R. Karplus and N. M. Kroll, Phys. Rev. **77**, 536 (1950).

[6] A. Petermann, Nuclear Phys. **3**, 689 (1957); **5**, 677 (1958); Helv. Phys. Acta **30**, 407 (1957).

[7] C. M. Sommerfield, Phys. Rev. **107**, 328 (1957); Ann. Phys. **5**, 26 (1958).

ments of μ_e/μ_p have been performed.[8–11] These determinations are consistent to approximately one ppm. The Gardner and Purcell result may be combined with the μ_e/μ_p data of Beringer and Heald[9] (see Sec. 12) to yield for the electron moment

$$\mu_e/\mu_0=1+(\alpha/2\pi)-(2.5\pm2.3)(\alpha^2/\pi^2)$$
$$=1.001148\pm0.000012(\sim12\text{ ppm}), \quad (2.2)$$

where the uncertainty represents the limit of error. When we use our determination of μ_p/μ_0 (see Sec. 11), we obtain for the magnetic moment of the free electron

$$\mu_e/\mu_0=1+(\alpha/2\pi)+(1.2\pm0.9)(\alpha^2/\pi^2)$$
$$=1.001168\pm0.000005(\sim5\text{ ppm}), \quad (2.3)$$

where the uncertainty represents the estimated 50% probable error.

3. OUTLINE OF THE EXPERIMENT AND PREVIOUS MEASUREMENTS

The nuclear magnetic resonance frequency $\omega_p=2\mu_{p(\text{oil})}H/\hbar$ of protons in mineral oil and the cyclotron frequency $\omega_e=eH/mc$ of free low-energy electrons are measured in the same magnetic field H. The ratio of these two frequencies yields the proton moment in Bohr magnetons, $\omega_p/\omega_e=\mu_{p(\text{oil})}/\mu_0$, uncorrected for environmental shifts due to the mineral oil. The difficulties in this type of experiment are largely associated with the measurements related to the electron cyclotron resonance.

In the Gardner and Purcell experiment[2] the electron cyclotron resonance was observed in a magnetic field of approximated 3340 gauss, at which field the electron resonance frequency is approximately 9360 Mc/sec. An evacuated rectangular wave guide, its broad dimension parallel to the magnetic field, was traversed by a low-energy space charge limited ribbon-like beam of electrons. The electrons were injected into the guide through a narrow slit in the guide wall; as the electrons drifted across the guide, in a direction parallel to the external magnetic field, they were subjected to the transverse electric component of the microwave field within the guide. The electron current was collected and measured subsequent to its departure through a narrow slit in the far wall of the guide. An almost hundred-fold increase in collected electron current was observed for microwave frequencies in the neighborhood of the electron cyclotron frequency. The interpretation of this effect was that the electron space charge was expanded by the microwave field, thus reducing the current-limiting space charge potentials within the guide. The electron cyclotron frequency was interpreted to be that frequency of the microwave field at which the collected electron current was a maximum. In the Nelson[2] modification of this experiment the above kinematical detection scheme was discarded in favor of monitoring the microwave power absorbed by the electron beam.

In the present experiment a microwave absorption technique was applied to a sample of free electrons contained in a highly evacuated spherical bulb of Pyrex ~0.7 cm in diameter. The electrons were produced by photoelectric emission from the surface density equivalent of a film of a few molecular layers of potassium deposited upon the inner surface of the sphere.[12]

One of the important limitations on accuracy in the Gardner and Purcell experiment was imposed by possible shifts in the electron cyclotron frequency arising from the presence of inhomogeneous electrostatic fields. These fields can be produced by space charge, externally applied trapping voltages, or stray charges accumulating on the boundaries of the system within which the resonance is studied. The present experiment is designed to correct for these shifts in a fashion that does not require a quantitative knowledge of the electrostatic field distribution.

We make three assumptions which are subject to experimental verification: (1) the electron orbit radii are small compared to distances in which the electrostatic field varies appreciably; (2) the frequency shift caused by the electrostatic field is small; (3) the electrostatic field is independent of magnetic field in a chosen range of magnetic field variation.

When assumptions (1) and (2) obtain it can be shown (see Sec. 6) that the experimentally observed frequency ratio ω_e'/ω_p is related to $\mu_0/\mu_{p(\text{oil})}$ by the expression

$$\omega_e'/\omega_p=[\mu_0/\mu_{p(\text{oil})}][1+(K/H^2)], \quad (3.1)$$

where H is the magnetic field and K is a function only of the electrostatic field distribution. The absence of any electron orbit or velocity parameters in (3.1) suggests the measurement of ω_e'/ω_p as a function of magnetic field. If assumption (3) is satisfied one should observe a linear dependence of ω_e'/ω_p with respect to $1/H^2$. Thus a linear extrapolation to $1/H^2=0$ would determine $\mu_0/\mu_{p(\text{oil})}$.

We have studied ω_e'/ω_p as a function of $1/H^2$ for magnetic fields ranging from 750 to 1700 gauss. For each run, from three to thirteen points were taken in this interval. We have found, by analysis of all the data without rejection, that any systematic deviations from a straight line dependence are, in this interval, less than one part in one million.

4. FREE ELECTRON CYCLOTRON RESONANCE

We wish now to investigate the microwave power absorption exhibited by a cloud at free electrons in a magnetic field H. The physical system to which this analysis will be applied has the following pertinent features: The sample consists of 10^4-10^5 free electrons

[8] Koenig, Prodell, and Kusch, Phys. Rev. **88**, 191 (1952).
[9] R. Beringer and M. A. Heald, Phys. Rev. **95**, 1474 (1954).
[10] Geiger, Hughes, and Radford, Phys. Rev. **105**, 183 (1957).
[11] E. B. D. Lambe, Ph.D. thesis, Princeton University, 1959 (unpublished).

[12] One of us (P.F.) is very grateful for his conversation with Professor Purcell in 1951 in which several problems associated with this experiment were discussed.

contained within a $\sim\frac{1}{2}$ cm i.d. highly evacuated spherical Pyrex bulb. The electrons are continuously photoejected from a transparent potassium film upon the inner wall, with kinetic energies of ~ 1 ev corresponding to speeds of $\sim 5\times 10^7$ cm/sec. Mean electron lifetimes are observed to be $\sim 10^{-6}$ sec. The applied static magnetic field ranges from 750 to 1700 gauss. In a magnetic field of 1000 gauss the maximum diameters of the helical trajectories are $\sim 6\times 10^{-3}$ cm, or about 1/100 of the bulb diameter. The samples were evacuated to $\sim 3\times 10^{-8}$ mm of Hg. The amplitude of the microwave electric field was maintained at less than 10^{-3} volt/cm.

In this section we shall neglect the mutual interaction of the electrons and the influence of external static electric fields. Space charge and collective effects are discussed in Sec. 6. Relativistic corrections are treated in Sec. 10b.

Let the z axis of a rectangular coordinate system be aligned in the direction of the static magnetic field, and let E_x, E_y, and E_z be the components of the microwave electric field. The nonrelativistic equations of motion of an electron (charge $-e$) are, in Gaussian units,

$$dv_x/dt=-(e/m)(E_x+v_yH/c), \tag{4.1}$$

$$dv_y/dt=-(e/m)(E_y-v_xH/c), \tag{4.2}$$

$$dv_z/dt=-(e/m)E_z. \tag{4.3}$$

It can be demonstrated[13] that the E_z component of the microwave field employed in this experiment is responsible for a shift of less than 1 part in 10^{12} of the resonance frequency. We shall therefore neglect (4.3) and treat the problem as two dimensional.

It is convenient to introduce a complex velocity

$$V=v_x+iv_y,$$

and a complex electric field

$$\mathcal{E}=E_x+iE_y,$$

in terms of which Eqs. (4.1) and (4.2) can be combined to yield

$$dV/dt-i\omega_eV=-(e/m)\mathcal{E},$$

or

$$(d/dt)(Ve^{-i\omega_et})=-(e/m)\mathcal{E}e^{-i\omega_et}, \tag{4.4}$$

where $\omega_e\equiv eH/mc$.

Let us now represent the microwave electric field by

$$\mathcal{E}=E\sin(\Omega t+\varphi), \tag{4.5}$$

where E, assumed without loss of generality to be real, is the amplitude of the field, Ω is the circular frequency of the electric field, and φ is a phase factor, Equation (4.4) can be integrated, upon the substitution of (4.5), to yield

$$Ve^{-i\omega_et}=V_0+\frac{eE}{2m}\left(\frac{e^{i(\Omega-\omega_e)t}-1}{\Omega-\omega_e}e^{i\varphi}+\frac{e^{-i(\Omega+\omega_e)t}-1}{\Omega+\omega_e}e^{-i\varphi}\right), \tag{4.6}$$

where V_0 is the complex velocity of the electron at time $t=0$.

The change in the kinetic energy of the electron is given by

$$\Delta w=\tfrac{1}{2}m(V^*V-V_0{}^*V_0), \tag{4.7}$$

where V^* is the conjugate complex velocity at time t and $V_0{}^*$ is the conjugate complex velocity at $t=0$. If we substitute (4.6) into (4.7) and let $V_0=v_0{}^{i\theta}$, where v_0 is real, we obtain

$$\Delta w=mv_0\left(\frac{eE}{2m}\right)\left(\frac{\cos[(\Omega-\omega_e)t+\varphi-\theta]-\cos[\varphi-\theta]}{\Omega-\omega_e}+\frac{\cos[(\Omega+\omega_e)t+\varphi+\theta]-\cos[\varphi+\theta]}{\Omega+\omega_e}\right)$$

$$+2m\left(\frac{eE}{2m}\right)^2\left[\frac{\sin^2\tfrac{1}{2}(\Omega-\omega_e)t}{(\Omega-\omega_e)^2}+\frac{\sin^2\tfrac{1}{2}(\Omega+\omega_e)t}{(\Omega+\omega_e)^2}\right]$$

$$+m\left(\frac{eE}{2m}\right)^2\left(\frac{\cos2\varphi+\cos2(\Omega t+\varphi)-\cos[(\Omega+\omega_e)t+2\varphi]-\cos[(\Omega-\omega_e)t+2\varphi]}{(\Omega-\omega_e)(\Omega+\omega_e)}\right). \tag{4.8}$$

The sample contains a large number of electrons, and we shall require an expression for the average energy absorbed per electron. Since there is no correlation between the rate of electron emission and the phase of the microwave field,[14] Eq. (4.8) must be averaged over φ to obtain for the average energy absorbed by an electron living for a time t

$$\langle\Delta w\rangle_{\text{Av}}=\frac{(eE)^2}{2m}\left[\frac{\sin^2[\frac{1}{2}(\Omega-\omega_e)t]}{(\Omega-\omega_e)^2}+\frac{\sin^2[\frac{1}{2}(\Omega+\omega_e)t]}{(\Omega+\omega_e)^2}\right]. \tag{4.9}$$

It will be noted that (4.9) is independent of the initial magnitude v_0 and direction θ of the electron velocity; this feature enables the microwave power absorption P to be expressed in terms of the above average (4.9), the number of electrons emitted per second N, and the

[13] S. Liebes, Jr., reference 1.

[14] It can be shown that such a correlation could, for the observed resonances, give rise to a shift in the resonance frequency of at most one part in 10^{12}.

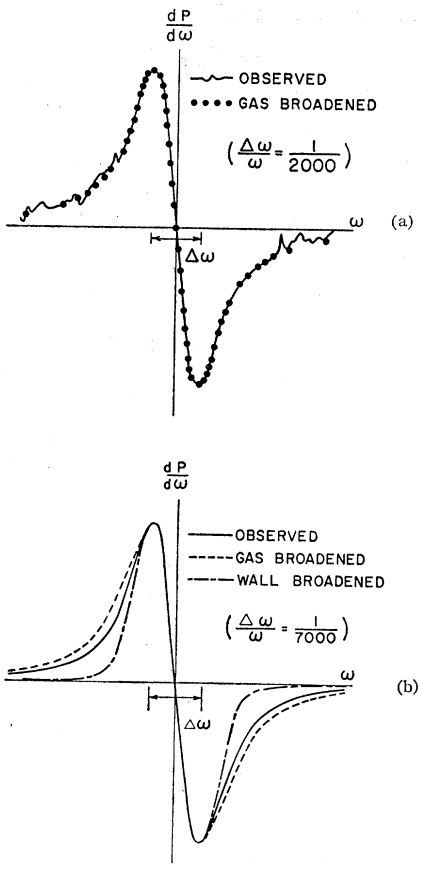

FIG. 1. In (a) the frequency derivative of an observed gas collision broadened electron resonance is compared with the derivative of the associated theoretically obtained Lorentzian line shape (4.13). The signal-to-noise ratio for this gassy bulb was unusually poor. In (b) the frequency derivative of a typical one of the electron power absorption curves is compared with derivatives of (4.13) and (4.15), the latter representing a simplified model of wall collision broadening.

normalized electron lifetime distribution function $L(t)$:

$$P=N\int_0^\infty \langle \Delta w\rangle_{\text{Av}} L(t)dt, \tag{4.10}$$

where $L(t)dt$ is that fraction of the electrons which have a lifetime between t and $t+dt$.

The second term on the right-hand side of (4.9) is antiresonant. It is straightforward to show[13] that, for the case of a relative line width small compared to unity, the inclusion of this term into the evaluation of (4.10) causes the power absorption maximum to experience a relative frequency shift given by

$$\frac{\delta\omega_e}{\omega_e}=-\frac{3}{\omega_e{}^4\langle t^4\rangle_{\text{Av}}},$$

where

$$\langle t^4\rangle_{\text{Av}}\equiv\int_0^\infty t^4 L(t)dt.$$

In the present experiment the values of ω_e and $\langle t^4\rangle_{\text{Av}}$ are such that $|\delta\omega_e/\omega_e|\ll 10^{-13}$. We therefore neglect the antiresonant term and obtain, upon substitution of the resonant part of (4.9) into (4.10), for the frequency dependence of the power absorption

$$P=N\frac{(eE)^2}{2m}\int_0^\infty \frac{\sin^2[\frac{1}{2}(\Omega-\omega_e)t]}{(\Omega-\omega_e)^2}L(t)dt. \tag{4.11}$$

Expression (4.11) shows that for the conditions considered, *maximum power absorption occurs for* $\Omega=\omega_e$ *and the power absorption curve is symmetric in* $(\Omega-\omega_e)$, *regardless of the form of* $L(t)$.

Expression (4.11) may be fitted to the experimental line shapes by the selection of a suitable distribution function $L(t)$. The true $L(t)$ will be an exceedingly complicated function of the geometry, the lighting conditions, the bulb surface conditions, etc. We make no attempt to develop a detailed theory of lifetime distribution functions. Our practical concern is that the resonances be symmetric; evidence providing support for the assumed symmetry of the resonance is presented in the discussion of measurement procedure (Sec. 9). Below we compare two of the observed line shapes with the very simplest of theoretical models.

One simple lifetime distribution function is that which approximates the case of gas (g) collision broadening:

$$L_g(t)=(1/\tau_g)e^{-t/\tau_g}. \tag{4.12}$$

The result of the substitution of (4.12) into (4.11) is the Lorentzian line shape

$$P_g=\alpha\tau_g{}^2/(1+x^2), \tag{4.13}$$

where $\alpha=N(eE)^2/4m$ and $x=(\Omega-\omega_e)\tau_g$, and τ_g is the mean electron lifetime.

The resonances were not generally gas collision broadened. However, one of the electron bulbs, which was constructed from fused quartz, had a thin wall (thickness $\sim$0.003 in.). A few months after the preparation of this sample, sufficient helium from the atmosphere had diffused into the bulb to give rise to a nearly Lorentzian line. A comparison of the frequency derivative of the power absorption curve for this bulb with the derivative of the Lorentzian line (4.13) is shown in Fig. 1(a). The curves have been matched at the points of inflection of the power absorption curve.

A simple model corresponding to a form of wall (w) collision broadening is that which corresponds to electrons being isotropically emitted, with a fixed initial speed v, from a plane wall into a uniform force field of strength eE directed toward this wall. The lifetime distribution function appropriate to this model is

$$\begin{aligned} L_w(t)&=1/\tau_w, \quad 0\leqslant t\leqslant\tau_w \\ &=0, \quad t>\tau_w, \end{aligned} \tag{4.14}$$

where $\tau_w=2mv/eE$ is the lifetime of an electron emitted in a direction normal to the wall. The line shape corre-

sponding to this model is

$$P_w=(\alpha\tau_w{}^2/x^2)[1-(\sin x/x)]. \tag{4.15}$$

It is not suggested that the model that lead to (4.15) corresponds closely to the actual physical situation. But for comparison purposes, there is shown in Fig. 1(b) one of the observed power absorption curve derivatives along with the derivatives of (4.13) and (4.15); the curves are matched together at the inflection points of the power absorption curve.

5. QUANTUM MECHANICAL CONSIDERATIONS

The electrons in this experiment have kinetic energies of ~ 1 ev, and hence maximum angular momenta of $\sim 10^6\hbar$ in a magnetic field of ~ 1000 gauss. We wish to show that, in the limit of vanishingly weak microwave fields, the result of the quantum mechanical calculation for the power absorbed by a cloud of low-energy cyclotroning electrons is precisely the same as that obtained by the classical methods of Sec. 4.

We require a set of energy eigenfunctions descriptive of an electron in a homogeneous magnetic field H_0; the Hamiltonian is of the form

$$\mathcal{H}_0=(1/2m)(\mathbf{p}+e\mathbf{A}/c)^2; \quad e>0. \tag{5.1}$$

A particularly convenient set is that given by Peierls[15]; an asymmetric gauge ($A_x=0$, $A_y=H_0x$, $A_z=0$) is exploited to obtain eigenfunctions having an harmonic oscillator dependence on x. The energy eigenvalues are equally spaced by the energy $W_n-W_{n-1}=\hbar\omega_e$.

At time $t=0$ let us turn on a weak microwave electric field:

$$E_x=E\sin(\Omega t+\varphi), \quad E_y=0, \quad E_z=0.$$

The total Hamiltonian then becomes

$$\mathcal{H}=\mathcal{H}_0+\mathcal{H}',$$

where $\mathcal{H}_0$ is given by (5.1) and

$$\mathcal{H}'=eEx\sin(\Omega t+\varphi).$$

If the electron is in a particular state $u_m(r)$ at time $t=0$, then at a later time t the probability that it will be found in the state $u_k(r)$, $k\neq m$ is given, in the weak-field limit, by

$$|a_k{}^{(1)}(t)|^2=\frac{(eE)^2}{m\hbar\omega_e}G_{km}{}^2\left(\frac{\sin^2[\frac{1}{2}(\Omega-\omega_{km})t]}{(\Omega-\omega_{km})^2}+\frac{\sin^2[\frac{1}{2}(\Omega+\omega_{km})t]}{(\Omega+\omega_{km})^2}\right.$$
$$\left.+\frac{1}{2}\frac{\cos 2\varphi+\cos[2(\Omega t+\varphi)]-\cos[(\Omega+\omega_{km})t+2\varphi]-\cos[(\Omega-\omega_{km})t+2\varphi]}{(\Omega-\omega_{km})(\Omega+\omega_{km})}\right); \tag{5.2}$$

$$G_{km}=\begin{cases}[(m+1)/2]^{\frac{1}{2}}, & k=m+1\\ (m/2)^{\frac{1}{2}}, & k=m-1\\ 0, & \text{otherwise}\end{cases}, \qquad \omega_{km}=(W_k-W_m)/\hbar.$$

In this calculation we have used the ordinary first order time dependent perturbation theory,[16] the $u_n(r)$ given by Peierls,[15] and the harmonic oscillator matrix elements.[17] We now average (5.2) over φ, all values of which are equally likely, to obtain

$$\langle|a_k{}^{(1)}(t)|^2\rangle_{\text{Av}}=\frac{(eE)^2}{m\hbar\omega_e}G_{km}{}^2\left[\frac{\sin^2[\frac{1}{2}(\Omega-\omega_{km})t]}{(\Omega-\omega_{km})^2}+\frac{\sin^2[\frac{1}{2}(\Omega+\omega_{km})t]}{(\Omega+\omega_{km})^2}\right]. \tag{5.3}$$

The average value of the energy absorbed by an electron living for a time t is then

$$\langle\Delta w\rangle_{\text{Av}}=\hbar(\langle|a_{m+1}{}^{(1)}(t)|^2\rangle_{\text{Av}}-\langle|a_{m-1}{}^{(1)}(t)\rangle_{\text{Av}})$$
$$=\frac{(eE)^2}{2m}\left[\frac{\sin^2[\frac{1}{2}(\Omega-\omega_e)t]}{(\Omega-\omega_e)^2}+\frac{\sin^2[\frac{1}{2}(\Omega+\omega_e)t]}{(\Omega+\omega_e)^2}\right]. \tag{5.4}$$

This expression has been developed for arbitrary initial conditions and for a very weak microwave field; it contains no quantum parameters and is identical to the classical result given in Sec. 4, Eq. (4.9).

6. MUTUAL ELECTRON INTERACTIONS AND STATIC ELECTRIC FIELDS

We wish to consider the effects which static electric fields and the mutual interactions of the electrons have upon the cyclotron resonance. These effects consist of small but significant shifts of the cyclotron resonance frequency. The magnetic perturbations arising from the 10^4-10^5 electrons are several orders of magnitude below the sensitivity of the experiment so that this discussion will be confined to an analysis of the electric terms only. We treat the interaction of a single electron with its neighbors in the sample from the macroscopic space charge point of view; the lifetime of the electrons which contribute significantly to the resonance is very large in comparison to the period of rotation in an orbit.

We first note that though a homogeneous static electric field will contribute to the average energy of an electron, this field will not appreciably affect either the

[15] R. Peierls, *Quantum Theory of Solids* (Clarendon Press, Oxford, 1955), p. 146.
[16] L. I. Schiff, *Quantum Mechanics* (McGraw-Hill Book Company, Inc., New York, 1949), first edition, Chap. 8.
[17] L. I. Schiff, reference 17, Chap. IV.

magnitude or the frequency dependence of microwave power absorption. A component of static electric field parallel to the magnetic field will accelerate the electron, but the transverse motion will be influenced only in so far as the mass of the electron is relativistically altered. A transverse component of static electric field will impart to the electron a skitter velocity in a direction mutually perpendicular to both the electric and magnetic fields. This skitter will not, however, give rise to a detectable alteration of the microwave power absorption.

An inhomogeneous static electric field can, however, cause a significant shift of the electron cyclotron frequency. In order to develop a general classical formulation[18] of this shift, let us transform to that frame of reference in which the local electron trajectories, when projected upon a plane normal to the magnetic field, are most nearly circular; we call this the "skitter frame." In this frame,

$$m\omega v_\perp = eE_r + (ev_\perp H/c), \quad e>0,$$

or

$$\omega = \omega_e[1+(E_r c/Hv_\perp)], \quad \omega_e \equiv eH/mc, \tag{6.1}$$

where $v_\perp$ is the instantaneous component of velocity perpendicular to the magnetic field, $\omega = d\theta/dt$ is the instantaneous component of angular velocity parallel to the magnetic field, and E_r is the static electric field component directed away from the instantaneous center of curvature of the projected orbit. We now average both sides of Eq. (6.1) over one period and obtain for the average angular velocity ω'

$$\omega' \equiv \frac{1}{T}\int_0^T \omega dt = \omega_e\left(1+\frac{1}{T}\int_0^{2\pi}\frac{E_r c}{Hv_\perp \omega}d\theta\right), \tag{6.2}$$

where T is the time required for θ to increase by 2π. The relative frequency shift is very small in the present experiment so that

$$\frac{1}{T}\int_0^{2\pi}\frac{E_r c}{Hv_\perp\omega}d\theta \ll 1.$$

We shall therefore approximate the integral in (6.2) by considering both $v_\perp$ and ω, each of which is nearly constant throughout the cycle, to be constants in the integration. We then obtain

$$\omega' = \omega_e[1+(\langle E_r\rangle_{\text{Av}} c/Hv_\perp)], \tag{6.3}$$

where

$$\langle E_r\rangle_{\text{Av}} = \frac{1}{2\pi}\int_0^{2\pi} E_r d\theta \tag{6.4}$$

is the average radial electrostatic field at the orbit.

In order to express $\langle E_r\rangle_{\text{Av}}$ in terms of the static electric field distribution and the orbit size, let us position a rectangular coordinate system at rest in the skitter frame with the origin located at the center of the electron orbit and with the z axis oriented in the direction of the magnetic field. In this frame

$$E_r(r,\theta) = E_x(r,\theta)\cos\theta + E_y(r,\theta)\sin\theta. \tag{6.5}$$

We assume that the electron orbit radii are sufficiently small, compared to distances in which the electrostatic field changes appreciably, that (6.5) may be approximated by the first terms of a power series expansion about the origin:

$$\begin{aligned} E_r(r,\theta) = \Big[& E_{x0} + \left(\frac{\partial E_x}{\partial x}\right)_0 r\cos\theta + \left(\frac{\partial E_x}{\partial y}\right)_0 r\sin\theta \\ & + \tfrac{1}{2}\left(\frac{\partial^2 E_x}{\partial x^2}\right)_0 r^2\cos^2\theta + \left(\frac{\partial^2 E_x}{\partial x\partial y}\right)_0 r^2\cos\theta\sin\theta \\ & + \tfrac{1}{2}\left(\frac{\partial^2 E_x}{\partial y^2}\right)_0 r^2\sin^2\theta + \cdots\Big]\cos\theta \\ & + \Big[E_{y0} + \left(\frac{\partial E_y}{\partial x}\right)_0 r\cos\theta + \left(\frac{\partial E_y}{\partial y}\right)_0 r\sin\theta \\ & + \tfrac{1}{2}\left(\frac{\partial^2 E_y}{\partial x^2}\right)_0 r^2\cos^2\theta + \left(\frac{\partial^2 E_y}{\partial x\partial y}\right)_0 r^2\cos\theta\sin\theta \\ & + \tfrac{1}{2}\left(\frac{\partial^2 E_y}{\partial y^2}\right)_0 r^2\sin^2\theta + \cdots\Big]\sin\theta. \end{aligned} \tag{6.6}$$

Substitution of (6.6) into (6.4) yields:

$$\langle E_r\rangle_{\text{Av}} = \tfrac{1}{2}r[(\partial E_x/\partial x)_0 + (\partial E_y/\partial y)_0]. \tag{6.7}$$

Expression (6.7) is valid through second order in r since all terms of even order vanish upon integration. The field derivatives may be evaluated either in the skitter frame or the laboratory frame since the electric fields seen in the two frames differ from one another only by a constant vector field.

Inserting (6.7) into (6.3), and making the substitution $v_\perp = eHr/mc$, we find that the electron will follow a cyclotron orbit at the circular frequency

$$\omega' = \omega_e\left\{1+\frac{mc^2}{2eH^2}\left[\left(\frac{\partial E_x}{\partial x}\right)_0 + \left(\frac{\partial E_y}{\partial y}\right)_0\right]\right\}, \tag{6.8a}$$

or equivalently,

$$\omega' = \omega_e\left\{1+\frac{mc^2}{2eH^2}\left[4\pi\rho_0 - \left(\frac{\partial E_z}{\partial z}\right)_0\right]\right\}, \tag{6.8b}$$

where ρ_0 is the local space change density.

The most important feature of (6.8a,b) is that the frequency shift is independent of the electron energy and orbit radius; the shift is determined entirely by the magnetic field and by the parameters of the electrostatic field. This feature permits the cyclotron frequency ω_e to

[18] See the Appendix for a quantum mechanical treatment of this shift.

be determined by an extrapolation procedure, the application of which does not require a quantitative description of the electrostatic field.

7. EXTRAPOLATION PROCEDURE

For convenience we rewrite (6.8) in the abbreviated form

$$\omega'=\omega_e[1+(mc^2/2eH^2)\Gamma],$$
$$\Gamma\equiv(\partial E_x/\partial x)_0+(\partial E_y/\partial y)_0=4\pi\rho_0-(\partial E_z/\partial z)_0. \quad (7.1)$$

Since the field term Γ is generally a function of position within the electron bulb, (7.1) expresses the spatial dependence of the frequency ω'. The fundamental problem is to relate the observed apparent cyclotron frequency ω_e', specifically the frequency at which maximum power is absorbed by the sample, to the desired unperturbed cyclotron frequency $\omega_e=eH/mc$.

We conclude from (4.11) that if each of the electrons in the sample is cyclotroning at the same frequency ω', then the power absorption curve is symmetric in $(\Omega-\omega')$ about the frequency $\Omega=\omega'$. We may represent such a curve by the expression

$$P(\Omega-\omega')=\psi[b(\Omega-\omega')^2], \quad (7.2)$$

where small values of the line width parameter b are associated with broad resonances.

We now develop a generalized form of (7.2) that is applicable to the experimental situation in which ω' is a function of position within the bulb. We wish to obtain an expression for $P(\Omega-\omega_e')$ where ω_e' is that frequency at which maximum absorption occurs in the sample. We denote the difference between the measured frequency ω_e' and the unperturbed classical cyclotron frequency ω_e by

$$\delta\omega\equiv\omega_e'-\omega_e, \quad (7.3)$$

and write (7.1) in the form

$$\omega'=\omega_e'-\delta\omega+(c/2H)\Gamma. \quad (7.4)$$

We introduce a normalized distribution function $\sigma(\Gamma)$ which is equal to the fraction of electrons per unit Γ experiencing a field term of the value Γ, and obtain from (7.1) and (7.2)

$$P(\Omega-\omega_e')=\int_{\Gamma_{\min}}^{\Gamma_{\max}}\psi\left[b\left(\Omega-\omega_e'+\delta\omega-\frac{c}{2H}\Gamma\right)^2\right]\sigma(\Gamma)d\Gamma. \quad (7.5)$$

It has been observed in the case of the present experiment that the primary resonance broadening mechanism is the electron lifetime distribution rather than the variation of Γ over the bulb. Thus, b is small enough to prevent the shape of the resonance from being controlled by $\sigma(\Gamma)$. We therefore seek the value of $\delta\omega$ in the limit that b tends toward zero. We first establish the value of $\delta\omega$ by differentiating both sides of (7.5) with respect to $(\Omega-\omega_e')$ and setting $\Omega=\omega_e'$. This procedure yields

$$\delta\omega=\int_{\Gamma_{\min}}^{\Gamma_{\max}}\psi'\left[b\left(\delta\omega-\frac{c}{2H}\Gamma\right)^2\right]\frac{c}{2H}\Gamma\sigma(\Gamma)d\Gamma \div\int_{\Gamma_{\min}}^{\Gamma_{\max}}\psi'\left[b\left(\delta\omega-\frac{c}{2H}\Gamma\right)^2\right]\sigma(\Gamma)d\Gamma, \quad (7.6)$$

where ψ' denotes the derivative of ψ with respect to its argument in (7.5). Letting b tend toward zero in (7.6) we find[19]

$$\lim_{b\to0}\delta\omega=\frac{c}{2H}\langle\Gamma\rangle_{\text{Av}},$$

where (7.7)

$$\langle\Gamma\rangle_{\text{Av}}=\int_{\Gamma_{\min}}^{\Gamma_{\max}}\Gamma\sigma(\Gamma)d\Gamma.$$

Thus, for an electric field induced frequency shift $\delta\omega$ which is small compared to the natural linewidth of the resonance, we have, from (7.3) and (7.7),

$$\omega_e'=\omega_e[1+(mc^2/2eH^2)\langle\Gamma\rangle_{\text{Av}}]. \quad (7.8)$$

The value of ω_e' is therefore not sensitive to the details in the structure $\sigma(\Gamma)$.

It will be recalled now (see Sec. 3) that $\omega_e/\omega_p=\mu_0/\mu_{p(\text{oil})}$; therefore, we obtain from (7.8)

$$\frac{\omega_e'}{\omega_p}=\frac{\mu_0}{\mu_{p(\text{oil})}}\left[1+\frac{mc^2}{2eH^2}\langle\Gamma\rangle_{\text{Av}}\right]. \quad (7.9)$$

If the electric field configuration within the bulb were known, we could determine the value of $\mu_0/\mu_{p(\text{oil})}$ from a single measurement of ω_e'/ω_p. It is not possible in practice, however, to obtain a detailed description of the field.

Inspection of (7.9) suggests the possibility of developing an experimental extrapolation procedure for the determination $\mu_0/\mu_{p(\text{oil})}$. If $\langle\Gamma\rangle_{\text{Av}}$ is insensitive to H, then a plot of values of ω_e'/ω_p *vs* $1/H^2$ should yield a straight line which when extrapolated to $(1/H^2)=0$ would establish the value for $\mu_0/\mu_{p(\text{oil})}$.

Let us consider the dependence of $\langle\Gamma\rangle_{\text{Av}}$ upon H. For magnetic fields in the neighborhood of 1000 gauss we have already noted that the electron orbit diameters are $\sim$100 times smaller than the bulb diameter. The kinematics of the emission of electrons from the spherical bulb surface is therefore expected to be little effected by changes of the value of the magnetic field for $H\sim1000$ gauss. Furthermore, since orbit radii are small compared to characteristic dimensions of the space charge (see Sec. 10A) a decrease in the size of the orbits will have very little effect upon the space charge distribution. However, the transverse skitter velocities of the electrons are sensitive to variations of the magnetic field,

[19] This result is a special case of a more general theorem that is to be discussed by P. Franken and G. Newell in a later paper.

and we must consider how far an electron may be expected to skitter as it crosses the bulb. The characteristic lifetime τ, for those electrons which contribute significantly to the resonance, is estimated from line width observations to be $\sim 3\times 10^{-7}$ sec. With at most $\sim 10^5$ electrons confined to the interior a bulb of radius $R\sim 0.3$ cm and distributed as described in Sec. 10A, space charge fields E_s as large as $\sim 10^{-3}$ esu could occur. Thus, at $H=10^3$ gauss, an electron might skitter a maximum distance of $(cE_s\tau/H)\sim 10^{-2}$ cm. We conclude that for magnetic field intensities of the order of 1000 gauss, the electric field term $\langle\Gamma\rangle_{\text{Av}}$ should be fairly independent of the magnetic field.

The extrapolation procedure suggested above has been adopted in the present experiment. The independence of $\langle\Gamma\rangle_{\text{Av}}$ upon the magnetic field intensity has been verified experimentally. The experiment has been designed to permit an investigation of the ratio ω_e'/ω_p over a range of magnetic fields from 750 to 1700 gauss. The measurements have been performed under an extreme variety of bulb lighting conditions, microwave power inputs, potassium distributions within the sample, gas pressures, etc.

The signs of the slopes obtained from plots of ω_e'/ω_p *vs* $1/H^2$ suggest that the value of $\langle\Gamma\rangle_{\text{Av}}$ was determined primarily by the electron space charge distribution. The space charge density within the electron bulb has been obtained by fitting (7.9) to the measured line slopes. The estimate of $n\sim 10^4-10^5$ for the number of electrons momentarily free within the bulb is based upon additional information regarding the spatial configuration of electron cloud. This value of n is in reasonable agreement with estimates obtained from microwave absorption measurements.

8. APPARATUS

A. Electron-Proton Head

The electron and proton frequency measurements could have been performed at different locations in the magnetic field, in conjunction with a determination of the ratio of the fields at the two sample sites. This method was considered impractical because measurements had to be taken over a relatively broad range of magnetic fields. The unavoidable magnetic field inhomogeneity was field sensitive and could be accurately reproduced only by careful cycling.

A common field technique was therefore adopted. A rapid and accurate interchange of samples in the magnetic field was accomplished by use of a mobile electron-proton (*e-p*) head. Measurements were taken with three different *e-p* head assemblies of the type illustrated in Fig. 2; one of brass, one of OFHC copper, and one of aluminum. The head consisted of a metal block into the vertical front face of which were bored two identical horizontal parallel holes, one to receive the electron sample, and one to receive the proton sample. An axial metal post extended part way forward from the rear wall of the electron bore hole. This bore hole functioned as a microwave cavity which was excited and monitored by the use of electric field coupling. The cavity was tuned in its lowest mode by an annular shorting plunger which established electrical contact with the cavity walls and the center post through flexible fingers of phosphor-bronze. The cavity was tunable from 2000 to 4500 Mc/sec, and the Q was ~ 500. The electron sample was placed on axis near the end of the center post; in this region the microwave electric field was approximately axial. The external steady magnetic field was directed normal to the large vertical side walls of the head and thus normal to the microwave electric field. The cylindrical portion of the cavity, extending forward from the front end of the center post, functioned as a section of wave guide beyond cutoff and provided a satisfactory aperture for the illumination of the electron sample.

The proton bore hole, the lower hole in Fig. 2, was fitted with one of several hollow Lucite coil forms upon which were wound approximately 15 turns of No. 24 bare copper wire. One end of this oscillator coil was grounded to the cavity wall and the other end was soldered to a $\frac{1}{8}$-in. diameter copper rod which extended through and was insulated from the rear wall of the bore hole.

The head was symmetrically designed so that the electron and proton subassemblies could each be inserted into either one of the cavity bore holes. This interchangability provided one means of testing the head for asymmetric magnetic contamination.

The electron and proton samples of nearly identical shape and size were clamped to a removable symmetric face plate which was fitted to a machined seat on the head. Alignment of the electron and proton samples was accomplished by fastening the face plate to a separate alignment jig. The slender sighting wires of the jig

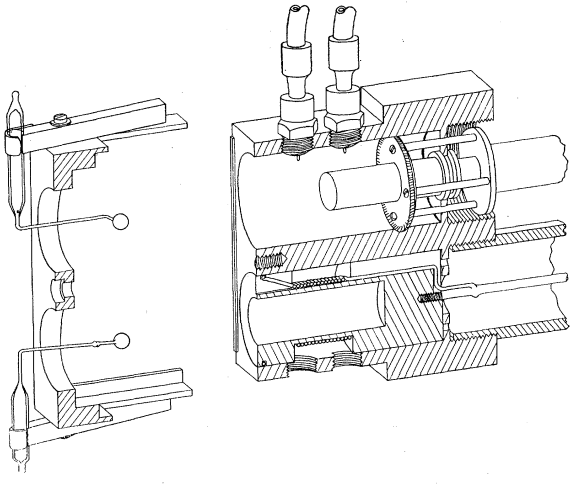

FIG. 2. Cross section of a typical one of the electron-proton heads. The face plate is shown separated from the head. Of the two samples clamped to the face plate, the upper one is the electron sample and the lower one is the proton sample.

enabled the sample centers to be reproducibly positioned within 0.01 in.

The electron and proton samples could be moved into their operating positions in the magnetic field by an eccentric drive and connecting rod mechanism which possessed a stroke equal to the sample separation in the *e-p* head. The driven end of the connecting rod was fastened to a brass collet which in turn supported a 1-in. o.d. copper tube that was screwed to the back of the *e-p* head concentric with the proton oscillator coil. The collet rode on two vertical guide tubes attached to the yoke of the electromagnet. This device permitted the head to be moved very rapidly in the vertical plane from one operating position to the other. The reproducibility of this interchange was ~0.002 in.

B. Electron Samples

The photoelectrons were generated within the interior of the spherical portion of samples of the type illustrated in Fig. 2. The samples were blown from Pyrex tubing. The base section served as a potassium reservoir and as a means for handling and clamping the sample. The connection between the base and the bulb was a ~1.5-mm i.d., ~50 mm long, tubular stem.

The electron samples were prepared by attaching the bases of several newly blown vessels onto a high vacuum system. The vessels were pumped down to $\sim 3\times 10^{-8}$ mm Hg and simultaneously baked at about 450°C for ~24 hours. Deposits of solid potassium, previously prepared and sealed into the vacuum system in proximity to the vessels, were then warmed with a flame, and a visible trace of potassium was worked into the reservoir of each of the samples. After an additional period of pumping, to allow the escape of volatile impurities, the vessels were sealed off at their bases and removed from the vacuum system.

A freshly prepared sample would not immediately display an electron resonance unless a deliberate effort was made to work a small portion of the potassium from the reservoir into the bulb. If a newly prepared vessel were permitted to cure at room temperature, several weeks were required before the electron resonance could be observed. This fact suggests that the required photoelectric surface consisted of the equivalent of at least a monolayer of potassium, since it would take approximately 2 weeks for a monolayer of atoms to diffuse from the reservoir into the bulb at the room temperature vapor pressure of potassium ($\sim 3\times 10^{-8}$ mm Hg). Further qualitative evidence for the extreme thinness of the films is that they were totally invisible. If a visible amount of potassium were worked into the bulb the electron resonance would generally disappear. It is presumed that the disappearance of the resonance when these thick films where present was in some cases due to a shielding of the microwave electric field, as a consequence of the relatively short electrical time constant of the then conducting bulb surface.[20] It is believed that the film might also on occasions have prevented the establishment of incidental trapping fields (see Sec. 8D).

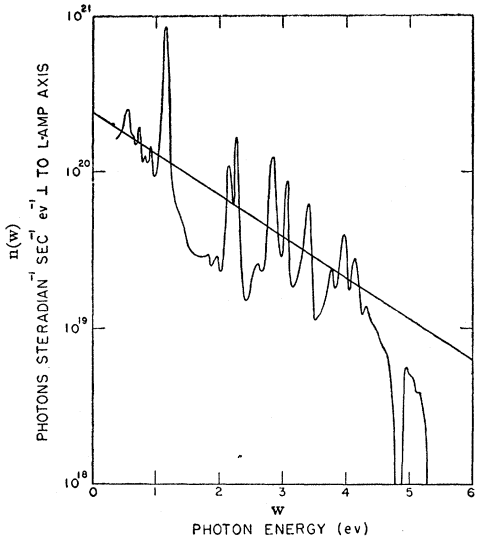

FIG. 3. Spectral distribution of radiation from air cooled *B-H6* mercury vapor lamp.

C. Proton Samples

To ensure geometrical symmetry of the electron and proton samples similar vessels were used to contain the electrons and the protons. For use as proton samples, the vessels illustrated in Fig. 2 were snapped at the stem near the bulb, and Squibb mineral oil (Heavy California Liquid Petrolatum) was injected into the spherical bulb. The broken stems were then reconnected. Vessels similarly filled with a 0.01-molal solution of $FeCl_3$ doped H_2O were compared with the mineral oil samples. The ratio of the nuclear magnetic resonance frequencies for the two different types of spherical samples was found to be $\omega(H_2O)/\omega_{(oil)}=1+(3.7\pm 0.40)\times 10^{-6}$, where the uncertainty represents the estimated 50% probable error.

D. Light Sources and Bulb Illumination

The electron cloud within the electron bulb was sustained by the process of photoelectric emission. Runs were taken by the use of either a 1000-watt air cooled General Electric *B-H6* mercury arc lamp or a 1000-watt incandescent projection lantern operating at a filament temperature of 3200°K. The data of this experiment were obtained for a variety of lighting intensities and distributions of illumination over the electron bulbs, though no alteration of lighting conditions was made during the course of any run. The term "run" is used in reference to any one of the series of measurements of ω_e'/ω_p taken at various values of magnetic field. The

[20] Further details are discussed by S. Liebes, Jr., reference 1.

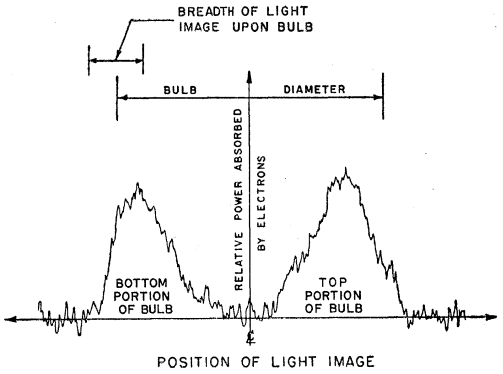

FIG. 4. Power absorbed by electrons as a function of electron bulb illumination configuration. The top-bottom sensitivity of the electron bulb is apparent from this plot of relative power absorbed by the electrons as a function of the vertical position of a horizontal band of light that has a vertical breadth of $\sim\frac{1}{5}$ of the electron bulb diameter. The static magnetic field is horizontally directed, perpendicular to incident beam of light. The source of illumination is the mercury vapor lamp.

most satisfactory runs were generally obtained with the use of the mercury lamp.

Figure 3 shows a plot of the number of photons emitted per ev per steradian per sec in a direction perpendicular to the lamp axis of the *B-H*6 mercury arc. The plot is characterized by pronounced spikes modulating a background which falls off approximately exponentially to $\sim$4 ev; the density then falls off more steeply to $\sim$5 ev beyond which energy the density may be considered, for practical purposes, to vanish. The straight line which is shown in the figure represents an exponential approximation to the spectral distribution; the equation for this line is

$$n(w)=2.3\times10^{20}e^{-w/1.63}, \tag{8.1}$$

where $n(w)$ is the number of photons emitted per ev per steradian per sec.

A most curious and unexpected phenomenon has been noted with regard to electron bulb illumination. It has been found that maximum electron power absorption generally occurred when either the top or the bottom portion of the electron bulb was illuminated by the external light source, as opposed to the case of uniform illumination of the entire electron bulb. The plot given in Fig. 4 shows the microwave power absorbed by the electrons as a function of the portion of the electron bulb illuminated by the mercury vapor lamp. A horizontal band of light having a vertical breadth of $\sim\frac{1}{5}$ of the electron bulb diameter was used to obtain this plot.

We feel inclined toward the following explanation of the above phenomenon. When only a portion of the bulb is illuminated, there is a pumping of electrons out of the illuminated into the neighboring unilluminated portion of the bulb. The relatively poor conductivity of the potassium deposit on the walls enhances the rapid attainment of an equilibrium static electric field distribution which only for the case of extreme top or bottom illumination, is of such a configuration as to favor electron trapping.

Trapping could be enhanced by placing a wire pigtail in the vicinity of the electron bulb in such an orientation as to not appreciably modify the cavity mode of oscillation. The pigtail was driven by an audio square wave of a few volts potential relative to ground. The incidence of the discontinuities in the square wave often provided a five or ten fold enhancement of the power absorption. This method of resonance enhancement was never employed in the course of data taking, since the details of the enhancement mechanism were not well understood.

E. Electronic Apparatus

A block diagram of the electronic apparatus used for the determination of the frequency ratio ω_e/ω_p is illustrated in Fig. 5.

The excitation for the electron cavity in the *e-p* head was derived from the 10th–30th harmonics of the internal crystal mixer of a Hewlett-Packard (H-P) 540-*A* Transfer Oscillator. The variable fundamental frequency of the oscillator, which covered the range 100–200 Mc/sec, was counted and digitally displayed by a H-P 524-*B* electronic counter used in conjunction with an H-P 525-*B* 100–220 Mc/sec frequency converter unit. The cavity possessed a sufficiently high Q ($\sim$500) to reject harmonics other than that to which it was tuned.

The amplitude of the oscillating electric field within the cavity was detected by a *SPR*-2 superheterodyne radar receiver. The receiver broadband audio output was approximately twenty times noise for the levels of oscillation employed. When the electron resonance frequency, determined by the magnetic field, was adjusted to center on the cavity frequency, the electric field amplitude dropped typically 15%. The receiver output signal-to-noise ratio for the electron resonance was thus $\sim$3. This latter figure was effectively improved to $\sim$100 by utilization of modulation and narrow band amplification.

The magnetic field at the sample site was modulated at 200 cps by 3-in. diameter coils fastened to the pole faces. The modulation amplitude was small compared to

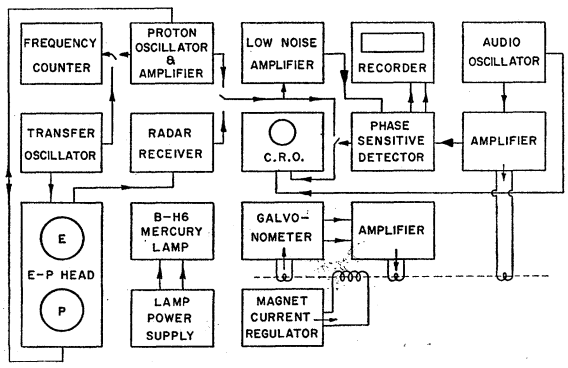

FIG. 5. Block diagram of electrical apparatus.

the electron resonance line width so that the 200-cps component of the receiver output was nearly proportional to the derivative of the electron power absorption curve. The receiver output was fed to a low-noise audio amplifier of gain 250, and thence to the 200-cps Q-multiplier section of a phase sensitive detector. The output of the Q-multiplier section was applied to the vertical input of a cathode-ray oscillograph. The magnetic field modulation was fed to the horizontal input of the oscillograph. Passage through resonance, which was accomplished by sweeping the magnetic field, produced a characteristic elliptic pattern upon the oscillograph.[21] The peak of the electron resonance manifested itself as a pattern of minimum vertical amplitude, the height of which, but for noise, would have been zero. It was found that this point could be reproducibly located to better than 1/100 of the electron linewidth. The derivative of the resonance curve could be traced by a Varian Associates model G-10 graphic recorder which was used in conjunction with the phase sensitive detector.

The proton sample was located in the *e-p* head proton bore hole directly beneath the electrons. The oscillation coil for the protons was connected to a sensitive regenerative oscillator derived from an audiofrequency Q-multiplier device discussed by Harris.[22] The oscillation, which was attenuated upon passage through resonance, was rectified and fed into the same modulation detection and display circuitry as was the electron signal. The magnetic field modulation was maintained the same for the detection of both the electron and the proton resonances. The center of the proton resonance could be reproducibly located to within one cycle per second.

The electromagnet and current regulator were early prototypes of the models currently produced by Varian Associates. The $7\frac{1}{2}$-in. diameter pole faces were separated by a gap of $1\frac{3}{4}$ in. The magnetic field was homogenized over the region of the samples by tilting the pole faces relative to the yoke of the electromagnet. In order to increase the field stability a device similar to the Varian Associates *V-K* 3500 Super Stabilizer was employed. In the course of running, the essentially linear drift of the magnetic field was generally less than 1 ppm/min.

9. MEASUREMENT PROCEDURE

The procedure followed in the course of a typical run will now be outlined. The electron and proton samples were secured to the *e-p* head face plate. The correct positioning of the samples on the face plate was accomplished by use of the alignment jig. The face plate was then fastened to the *e-p* head. An harmonic of the transfer oscillator was selected and adjusted to the frequency to which the cavity was tuned. The tuning operation was accomplished by either one of two methods. One method was to optimize cavity input and output coupling conditions, while at the same time maximizing the output of the radar receiver by performing fine adjustments of the transfer oscillator frequency. The tuning was accomplished while the magnetic field was so set that the electron cyclotron frequency was far removed from the cavity frequency. The other method relied upon the assumed symmetry of the electron resonance. The light was focused upon the electron sample, creating photoelectrons. The transfer oscillator was then adjusted so that the electron resonance, when observed by sweeping the magnetic field, displayed equal magnitudes for the derivatives at the inflection points on opposite sides of the power absorption curve. This latter procedure relied upon the assumption that any apparent asymmetry of the electron resonance was indicative of mistuning of the cavity. The fact that the same values were obtained for ω_e/ω_p in the extrapolation to infinite magnetic field, by use of each of the above tuning procedures, gives strong support to the assumption that no significant asymmetry existed in the electron resonance.

After completion of the electron cavity tuning, the magnetic field was adjusted to that value which yielded maximum electron cyclotron power absorption. The magnetic field stabilizer was then activated and the nuclear magnetic resonance oscillator was adjusted to the proton resonance frequency corresponding to the selected value of magnetic field. To measure the electron-proton frequency ratio at the particular magnetic field setting, a final adjustment of the transfer oscillator was made to compensate for any small magnetic field or oscillator drifts and the transfer oscillator frequency was counted. The proton sample was then rapidly moved into the position just occupied by the electrons. Final adjustment of the proton oscillator was made, and its frequency was counted. This operation was repeated so that a sandwich of five electron readings with four interposed proton readings was obtained in a total elapsed time of about two minutes. The entire procedure was then repeated at several different values of magnetic field in order to provide the data for a complete run.

The total of forty-two runs that were taken each contained from three to thirteen individual magnetic field dependent observations of ω_e'/ω_p. The order in which the values of magnetic field were chosen within any particular run was randomized in order to minimize the effects of possible systematic drifts. Frequently the first point was repeated at the end of the run in order to check for the occurrence of such drifts; no systematic drifts were detected.

[21] This detection technique is almost identical to that described in reference 8.

[22] H. E. Harris, Electronics (May 1951), p. 130. For our application this circuit was modified for radio-frequency operation and it performed as a sensitive oscillator when the regenerative feedback was adjusted to a high value.

10. CORRECTIONS AND UNCERTAINTIES

A. Magnetic Contamination Correction

A brass, an OFHC copper, and an aluminum electron-proton head were constructed for this experiment. Early in the course of the work, these pieces were tested for possible magnetic contamination. The procedure involved the placement into the electron bore hole of a Lucite form, a coil, and a mineral oil sample identical to those situated in the proton bore hole. By utilizing the sample interchange mechanism the nuclear magnetic resonance frequency within each bore hole could be measured at the same location in the magnetic field. The proton resonance frequencies at the sample sites in each hole were, for each of the electron-proton heads, in agreement to the order of 1 ppm. This was regarded as adequate evidence for magnetic purity, within the anticipated precision of the experiment. The brass cavity was easier to operate, owing to geometrical considerations and to the greater ease of tuning of the microwave components; this cavity was therefore used for most of the runs.

After the experiment was largely completed it was discovered, by means of an independent proton resonance probe, that the brass head had a more severe case of contamination than we had naively been lead to believe. Although the magnetic field, averaged over the sample volumes, was roughly the same in each bore hole, there was a large inhomogeneity of the field in each hole due to a bulk contamination of the brass. This contamination could readily have been corrected for if the electron resonance had taken place uniformly over the entire bulb, because in that case the electrons and protons would experience the same average field.[23] However, the experimental evidence discussed in Sec. 8D indicates that the electron resonances were observed over only a portion, top or bottom, of the electron bulb. Therefore, whereas the proton resonance corresponded to an average of the magnetic field over the entire bulb volume, the electron resonance corresponded to an average of the field over a fraction of the bulb volume, and a correction to the ω_e/ω_p measurements must be estimated.

These corrections have been obtained in a tedious but straightforward way.[24] The field distribution was measured over the sample sites by utilizing the two proton resonance assemblies; one oil sample was held fixed at the center of one bore hole and the other was moved to different locations in the other bore hole. The fields were compared at these different locations by means of the interchange mechanism. The fields were nominally the same for each bore hole and had a saddle like configuration roughly symmetric about a plane passing through the center position of the bore hole and parallel to the magnet pole faces. The field gradients in the sample volumes were as large as 5 ppm per millimeter, some five times greater than the field inhomogeneities produced by the magnet. Three dimensional field plots were obtained at 750 and 1500 gauss and were reproducible. Since the measurements were made with finite sized proton samples it was necessary to fit a point function to the data. This was done by expanding through quadratic terms in rectangular coordinates about the bulb centers.

TABLE I. Magnetic corrections for brass electron-proton head.

Illumination	Corrections to be applied to the ω_e/ω_p intercepts of each run[a]
Top of bulb	-0.0065 ± 0.0020
Bottom of bulb	-0.0050 ± 0.0020
No illumination information	-0.0057 ± 0.0025

[a] The uncertainties represent the estimated 50% probable error interval for these corrections. Note that $0.0006\cong1$ ppm.

From the experiments described in Sec. 8D, it was established that the electron resonances took place over either the top or bottom ~1 mm high regions of the electron bulb, depending upon the distribution of the illumination. For most of the data it was not known whether the top or the bottom sections were illuminated. The corrections were determined by computing the change produced in the slopes and positions of the "straight lines" of all runs by the field inhomogeneity. These corrections, which are listed in Table I, amount to ~10 ppm. Fortunately, the corrections required for top and bottom illuminations are nearly the same. Hence, for those runs where the illumination information was not recorded, we have taken an average of these corrections.

The 50% probable error interval for the majority of the corrections is taken to be ±0.0025 (~3 ppm) corresponding to an unknown distribution of illumination. It should be emphasized that this probable error estimate is a matter of our judgment. We explored a number of variations in experimental conditions, on paper and in the laboratory, in order to determine how sensitive the corrections were to bulb illumination and positioning. It is from this sort of "manipulation" that we estimated the reliability of the corrections, which estimate is expressed by the 50% probable error interval.

The corrections listed in Table I are for the electron and proton apparatus situated in the P hole and E hole, respectively, where this notation refers to orientation stampings on the side of the head. A few runs were taken with the reverse configuration. For these runs no corrections are required because the field distributions are such as to provide an accidental cancellation in the correction calculations.

The field corrections for the copper and aluminum heads turned out to be negligible; therefore, no corrections are applied to the data taken with these assemblies.

The microwave fittings and supporting pieces near the

[23] The electron and proton resonance frequencies would be those corresponding to the *average* magnetic field for the case of natural line widths large compared with the inhomogeneity.

[24] The data and detailed calculations for these corrections are to be found in the thesis of S. Liebes, Jr., reference 1.

resonance sites were checked with a small proton resonance probe and were found to be uncontaminated.

B. Photoelectron Relativistic Correction

The kinetic energies of ~ 1 ev imparted to the electrons in the process of photoemission were responsible for relativistic shifts of the cyclotron frequency of ~ 2 ppm. This shift is comparable to the precision of the experiment and a correction must therefore be estimated.

The ionization potential for potassium atoms is 4.34 ev, and the work function for solid potassium is 2.26 ev. The photoemission properties of very thin films,[25,26] however, are sensitive to the thickness and backing of the films and are not necessarily characteristic of the bulk form.[27] Fortunately we shall only require an estimate of the average energy of the emitted electrons because the resonance linewidths are much larger than the relativistic frequency shifts.[19]

The glass optical components prevented the entrance of hard ultraviolet photons (energy >4.34 ev) into the sample bulb. Thus photoionization of the potassium vapor is precluded and all of the electrons may be considered to come from the surface photoemission.

For the case of illumination by the incandescent lamp we shall approximate the photon spectrum by that of a black body at the filament temperature of 3200°K. The number of photons emitted per cm^2 of filament surface per sec in the differential energy band dw in the neighborhood of the energy w is

$$n(w)dw=\frac{2\pi w^2}{h^3c^2}\frac{1}{e^{w/kT}-1}dw. \tag{10.1}$$

The average kinetic energy $\langle w_s\rangle_{\text{Av}}$ of the electrons within the space charge cloud is taken to be

$$\langle w_s\rangle_{\text{Av}}=\int_\varphi^\infty (w-\varphi)w^{-\frac{1}{2}}n(w)dw \div \int_\varphi^\infty w^{-\frac{1}{2}}n(w)dw, \tag{10.2}$$

where the $w^{-\frac{1}{2}}$ term weights electron lifetimes, in the inverse proportion to the speed of the electron. The surface work function φ is not known but is expected to be greater than 1 ev in which event $(\varphi/kT)>4$. Thus, the error made by neglecting the -1 in the denominator of (10.1), when substituting into (10.2), will be less than 2%. Accordingly, (10.2) becomes

$$\langle w_s\rangle_{\text{Av}}=\left[\int_\varphi^\infty w^{\frac{1}{2}}e^{-w/kT}dw \Big/ \int_\varphi^\infty w^{\frac{1}{2}}e^{-w/kT}dw\right]-\varphi \tag{10.3a}$$

$$=kT\left(\frac{(\frac{5}{2},\infty)!-(\frac{5}{2},x)!}{(\frac{3}{2},\infty)!-(\frac{3}{2},x)!}-x\right), \quad x\equiv\varphi/kT. \tag{10.3b}$$

Values for the incomplete factorial functions appearing in (10.3b) are tabulated.[28] For $(\varphi/kT)>4$, $\langle w_s\rangle_{\text{Av}}$ is quite insensitive to φ and it very nearly approaches its limiting value: $\lim_{\varphi\to\infty}\langle w_s\rangle_{\text{Av}}=kT=0.28$ ev. This model represents a simplification of fact. We estimate, however, that for the incandescent illumination there is 50% probability that the average energy of the emitted electrons lies within the range given by

$$\langle w_s\rangle_{\text{Av}}=0.3_{-0.1}{}^{+0.5}\text{ ev}. \tag{10.4}$$

In order to estimate the correction that is necessary for the case of mercury lamp illumination, we refer to the photon spectrum given in Fig. 3. We believe that the potassium surface work function is in the neighborhood of 2 ev. We estimate, upon consideration of the exponential background and the nature of the spikes in the mercury lamp photon spectrum, that the average energy of the electrons within the space charge cloud should lie, with about 50% likelihood, in the range given by

$$\langle w_s\rangle_{\text{Av}}=1.5\pm 0.5\text{ ev}. \tag{10.5}$$

In view of the lack of detailed information regarding the photoemission properties of the thin potassium layer, a relatively large probable error has been associated with the $\langle w_s\rangle_{\text{Av}}$ given in both (10.4) and (10.5).

The fractional relativistic shift of the cyclotron frequency for a particle of kinetic energy T is, for $(T/mc^2)\ll 1$,

$$\Delta\omega/\omega=-T/mc^2. \tag{10.6}$$

Thus, from (10.4) and (10.5) we obtain for the relativistic corrections to the extrapolated intercept value of ω_e/ω_p,

$$\text{relativistic correction}=\begin{cases}+0.0004_{-0.0002}{}^{+0.0006} \\ \quad\text{(incandescent illumination)}, \\ +0.0019\pm 0.0006 \\ \quad\text{(Hg vapor illumination)},\end{cases} \tag{10.7}$$

where $0.006\cong 1$ ppm and the limits represent the estimated 50% probable error intervals.

C. Miscellaneous Corrections

The electron resonance was examined over the working range of microwave power input, and it was confirmed that there was no detectable power-dependent (relativistic) shift of the cyclotron frequency.

As will be shown in Sec. 11, the assumed linear dependence of ω_e/ω_p upon $1/H^2$ has been verified to within 0.5 ppm. Furthermore we have noted that systematic asymmetries in the resonances must be responsible for shifts of less than 2 ppm. We have found no detectable shifts in either the electron or the proton resonances as a function of the amplitude of field modulation. We summarize these observations by a miscellaneous cor-

[25] A. L. Hughes and L. A. DuBridge, *Photoelectric Phenomena* (McGraw-Hill Book Company, Inc., New York, 1932), first edition.
[26] S. Dushman, Revs. Modern Phys. **2**, 381 (1930).
[27] W. S. Souder, Phys. Rev. **8**, 310 (1916).
[28] E. Jahnke and F. Emde, *Tables of Functions* (Dover Publication, Inc., New York, 1945), p. 269.

TABLE II. Average values of ω_e/ω_p obtained by four different methods of fitting a straight line to the data.

Method of fit	Average uncorrected value of ω_e/ω_p
(1) Visual	657.46411
(2a) Least squares, weight 1	657.46396
(2b) Least squares, weight $(1/H^2)^{-\frac{1}{2}}$	657.46402
(2c) Least squares, weight $(1/H^2)^{-1}$	657.46408

rection to ω_e/ω_p,

Miscellaneous correction

$$=+0.0000\pm0.0015(\sim 2.5 \text{ ppm}), \quad (10.8)$$

where the uncertainty is assigned the significance of a 50% probable error.

Other possible sources of error appear to be negligible. The electric field associated with the time variation of the magnetic field modulation is too weak to give rise to any appreciable interaction with the electrons. Completely insignificant shifts arise as a result of the coupling of the electron spin moment to the space charge. The spontaneous radiation by the accelerating electrons is also insignificant. The longitudinal component of the microwave electric field produces a shift in the resonance frequency of the order of one part in 10^{12}.

11. RESULTS

We have taken a total of forty-two runs. Each of the runs served the dual function of (1) contributing to the establishment of an extrapolated value of ω_e/ω_p, and (2) testing the validity of the straight line hypothesis. These runs individually contained from three to thirteen observations of ω_e'/ω_p at values of magnetic field ranging from 750 to 1700 gauss.

The extrapolated intercept values of ω_e/ω_p at $1/H^2=0$ have been determined by fitting a "best" straight line to the points of each run. For each run, these fits have been determined in four different fashions: (1) visually; and (2a) by the method of least squares, where the squares of the residuals have been weighted equally, (2b) weighted by $(1/H^2)^{-\frac{1}{2}}$, and (2c) weighted by $(1/H^2)^{-1}$. The least-squares fits were obtained by the use of an IBM type-650 computer. Weights (2b) and (2c) were chosen to favor more heavily the data taken at the higher magnetic fields, since the reduced relative line width at these fields permitted relatively more precise measurements to be made. Of the four types of fit, method (2b) is considered to be the most appropriate. However, it can be seen from a comparison of the fits listed in Table II that the final result is very insensitive to the method of fitting the data.

A summary of the operating conditions and of the results that were obtained in each of the forty-two runs is compiled in Table III. The run numbers indicated in column (A) are assigned in the chronological order of the runs. The first letter given in column (B) identifies the electron-proton head used for the run, namely, A = aluminum, B = brass, C = copper. The last two letters in column (B) indicate, in accordance with stampings on the face of the head, the orientation of the symmetric head; E/P implies that the E stamp was above the P, and the inverse orientation is denoted by P/E. The electron assembly was always in the upper cavity. Column (C) identifies the electron bulb used, by denoting the date on which the sample was prepared; the A, B, C, etc., identify different bulbs made on the same day. Column (D) indicates the nature of the light source, i.e., whether incandescent (inc.) or mercury (Hg); the letters T, B, and U indicate whether the top, bottom, or unknown portion of the electron bulb was illuminated. Column (E) gives, for the electron resonance at $\sim$1700 gauss, 10^{-3} times the inverse relative line width measured at the inflection points of the power absorption curve. Column (F) indicates in arbitrary units the average relative power input to the electron cavity. Column (G) shows the average percent of input power that is absorbed by the electrons. Column (H) indicates the number of magnetic field dependent frequency ratio ω_e'/ω_p determinations that were contained in the run. Column (I) indicates the slope of the straight line that is fitted to the data points on a plot of ω_e'/ω_p *vs* $(2\pi\times10^7/\omega_p)^2$, where ω_p is measured in rad/sec. Column (J) gives the uncorrected extrapolated values of ω_e/ω_p that are obtained by fitting a straight line (method 2b) to the ω_e'/ω_p data plotted *vs* $1/H^2$. Column (K) gives the completely corrected individual determinations of $\omega_e/\omega_p=\mu_0/\mu_{p(\text{oil})}$; the entries of column (K) are obtained by adding the previously discussed corrections, which are summarized in Table IV, to the entries of column (J).

The raw data intercepts of column (J) and the completely corrected intercepts of column (K) are both plotted in chronological sequence in Fig. 6. Figures 7, 8, and 9 have been prepared to show the details of a poor, a typical, and a good run, respectively, as judged on the basis of conformity to the straight-line hypothesis.

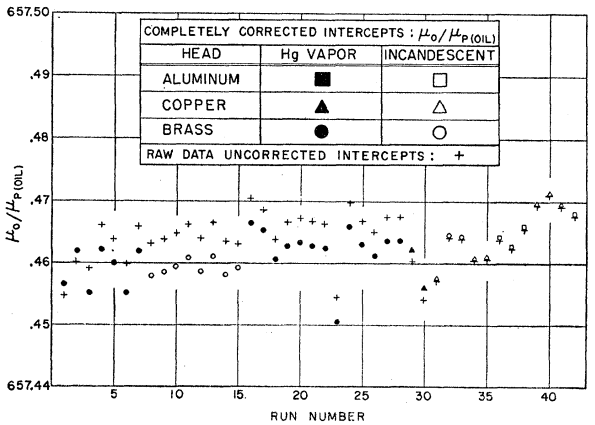

FIG. 6. Raw data and completely corrected results of the forty-two individual determinations of $\mu_0/\mu_{p(\text{oil})}$ plotted in chronological sequence.

TABLE III. A summary of the operating conditions and results obtained for each of the forty-two runs.

(A) Run	(B) e-p head and orient.	(C) Electron bulb	(D) Light and illum.	(E) $(\omega_e/\Delta\omega)$ $\times 10^{-3}$	(F) Average relative power input	(G) Average percent power absorp.	(H) No. points in run	(I) Slope $\frac{\Delta(\omega_e'/\omega_p)}{\Delta(2\pi\times 10^7/\omega_p)^2}$	(J) Raw intercept (ω_e/ω_p)	(K) Corrected intercept (ω_e/ω_p) $=\mu_0/\mu_{p(\text{oil})}$
1	*B-E/P*	12-3-55*C*	Hg-*U*	12	···	···	4	−0.0044	657.4546	657.4565
2	*B-E/P*	12-3-55*C*	Hg-*T*	15	···	···	7	−0.0034	657.4599	657.4618
3	*B-P/E*	12-3-55*C*	Hg-*U*	20	6	···	11	−0.0005	657.4589	657.4551
4	*B-P/E*	12-3-55*C*	Hg-*U*	11	6	···	7	−0.0052	657.4659	657.4621
5	*B-P/E*	12-3-55*C*	Hg-*U*	11	6	···	6	−0.0044	657.4637	657.4599
6	*B-P/E*	12-3-55*C*	Hg-*T*	18	6	···	13	−0.0041	657.4597	657.4551
7	*B-P/E*	12-3-55*C*	Hg-*U*	24	6	15	11	−0.0043	657.4656	657.4618
8	*B-P/E*	12-3-55*C*	inc.-*U*	24	6	6	7	−0.0039	657.4631	657.4578
9	*B-P/E*	12-3-55*C*	inc.-*U*	25	6	5	9	−0.0028	657.4637	657.4584
10	*B-P/E*	12-3-55*C*	inc.-*U*	20	6	6	4	−0.0025	657.4646	657.4593
11	*B-P/E*	12-3-55*C*	inc.-*U*	23	6	4	4	−0.0068	657.4660	657.4607
12	*B-P/E*	12-3-55*C*	inc.-*U*	30	4	15	4	−0.0009	657.4639	657.4586
13	*B-P/E*	12-3-55*C*	inc.-*U*	13	6	16	6	−0.0021	657.4663	657.4610
14	*B-P/E*	12-3-55*C*	inc.-*U*	11	6	16	6	−0.0014	657.4634	657.4581
15	*B-P/E*	12-3-55*A*	Hg-*U*	12	6	20	4	−0.0057	657.4630	657.4592
16	*B-P/E*	12-3-55*A*	Hg-*U*	17	4	10	4	+0.0002	657.4702	657.4664
17	*B-P/E*	12-13-55*C*	Hg-*B*	11	4	13	3	−0.0031	657.4683	657.4652
18	*B-P/E*	12-13-55*C*	Hg-*B*	13	2	20	6	−0.0031	657.4637	657.4606
19	*B-P/E*	12-13-55*A*	Hg-*U*	6	6	10	5	−0.0013	657.4664	657.4626
20	*B-P/E*	12-13-55*A*	Hg-*U*	14	6	10	4	−0.0011	657.4670	657.4632
21	*B-P/E*	12-13-55*A*	Hg-*U*	12	2	8	7	−0.0019	657.4665	657.4627
22	*B-P/E*	12-13-55*C*	Hg-*U*	7	6	15	8	−0.0042	657.4661	657.4623
23	*B-P/E*	12-13-55*C*	Hg-*U*	7	6	15	6	−0.0017	657.4543	657.4505
24	*B-P/E*	12-13-55*C*	Hg-*U*	···	···	···	4	−0.0042	657.4696	657.4658
25	*B-P/E*	12-13-55*C*	Hg-*U*	9	4	8	10	−0.0014	657.4667	657.4629
26	*B-P/E*	12-13-55*C*	Hg-*U*	10	2	5	4	−0.0006	657.4649	657.4611
27	*B-P/E*	12-13-55*C*	Hg-*U*	7	6	12	6	−0.0036	657.4673	657.4635
28	*B-P/E*	12-13-55*C*	Hg-*U*	8	4	13	6	−0.0069	657.4674	657.4636
29	*C-* —	12-13-55*C*	Hg-*U*	8	6	13	6	−0.0045	657.4602	657.4621
30	*C-* —	12-13-55*C*	Hg-*U*	6	9	35	4	−0.0042	657.4541	657.4560
31	*C-* —	12-13-55*C*	inc.-*U*	6	4	20	9	−0.0054	657.4571	657.4575
32	*B-E/P*	12-13-55*C*	inc.-*U*	17	4	13	9	−0.0020	657.4640	657.4644
33	*B-E/P*	12-13-55*C*	inc.-*U*	7	4	20	8	−0.0056	657.4638	657.4642
34	*C*-1/2	12-13-55*C*	inc.-*U*	8	1	15	13	−0.0030	657.4603	657.4607
35	*C*-1/2	12-13-55*C*	inc.-*U*	8	4	15	8	−0.0052	657.4606	657.4610
36	*A-E/P*	12-13-55*C*	inc.-*U*	7	4	14	6	−0.0026	657.4637	657.4641
37	*A-E/P*	12-13-55*C*	inc.-*U*	6	6	7	11	−0.0027	657.4622	657.4626
38	*A-E/P*	12-13-55*C*	inc.-*U*	10	6	9	12	−0.0025	657.4655	657.4659
39	*C*-1/2	12-13-55*C*	inc.-*U*	10	4	20	7	−0.0034	657.4692	657.4696
40	*C*-1/2	12-13-55*C*	inc.-*U*	10	2	15	5	−0.0032	657.4709	657.4713
41	*C*-1/2	12-13-55*C*	inc.-*U*	7	6	8	6	−0.0046	657.4690	657.4694
42	*A-E/P*	12-13-55*C*	inc.-*U*	7	6	20	6	−0.0024	657.4675	657.4679

Figure 10 shows the straight lines obtained in each of the forty-two runs. The slopes of these lines are those actually observed in the runs, but the lines have been vertically displaced to give the fully corrected intercept values presented in column (K) of Table III. The vertical dashed lines indicate the interval of magnetic field variation within which the data were taken.

Figure 11 has been prepared to test the straight-line hypothesis. The line shown in this figure represents, in the following sense, an average over all runs. Adjacent data points on the individual plots of each of the forty-two runs were first connected to one another by straight-line segments. Six equally spaced vertical lines were then constructed on the graph of each run at the magnetic field values represented by the abscissas of the points shown in Fig. 11. The points in this figure represent the averages of the intercepts obtained at the positions of each of the vertical lines on the individual graphs. The point at $(1/H^2)=0$ is the result of extrapolation and therefore does not have the same significance as the remaining five points. The straight line drawn through the six points misses none of these points by more than 2 ppm, the average departure being less than 0.5 ppm. The forty-two runs contain a total of 279 data points. The average departure of these points from the straight lines fitted to each run is 3.70 ppm. Thus, one would expect, on statistical grounds, that the average departure of the points in Fig. 10 should be ~0.57

TABLE IV. Summary of corrections.

Condition	Correction
Brass; top illumination of e bulb; P/E	−0.0065
Brass; unknown illumination of e bulb; P/E	−0.0057
Brass; bottom illumination of e bulb; P/E	−0.0050
Otherwise	0.0000
Incandescent lamp illumination	+0.0004
Mercury lamp illumination	+0.0019

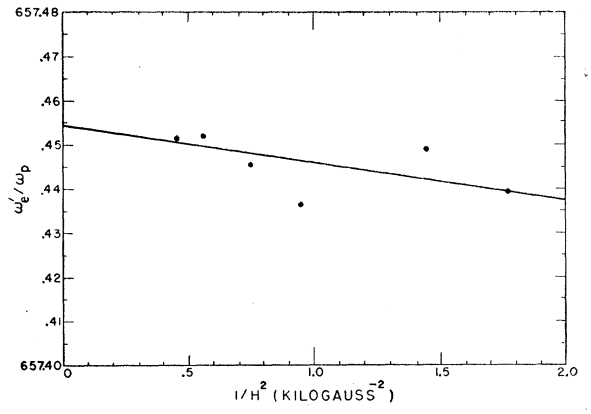

FIG. 7. Example of a poor run.

ppm; this value is to be compared with the observed 0.5 ppm. It is concluded that there is no significant systematic deviation from the predictions of the straight line hypothesis.

The average deviation of the forty-two completely corrected individual determinations of $\mu_0/\mu_{p(\text{oil})}$ is $a'=0.00316$ ($\sim$5 ppm) and the standard deviation of the completely corrected individual runs is $s'=0.00422$ ($\sim$6 ppm). The ratio $s'/a'=1.34$ may be compared with the value 1.25 that is to be expected for a large number of points in a normal distribution. It is evident however that a normal distribution is not to be expected in the present case, since none of the variable systematic errors can be precisely determined. The standard deviation of the average value is $s=0.00065$ ($\sim$1 ppm); this deviation is much smaller than the systematic uncertainties discussed in Secs. 10 A, B, and C.

Table V summarizes the independent estimated 50% probable errors that are associated with the individual corrections which are applied to the raw data.

The average of the results of the completely corrected individual determinations of $\mu_0/\mu_{p(\text{oil})}$ (listed in column K of Table III) is 657.4617. The estimated 50% probable error associated with this result is, from Table V, $P=(\sum P_i^2)^{\frac{1}{2}}=0.003$. We obtain then for protons observed in a spherical sample of mineral oil (Squibb Heavy California Liquid Petrolatum)

$$\mu_0/\mu_{p(\text{oil})}=657.462\pm0.003 \text{ (50\% probable error).} \quad (11.1)$$

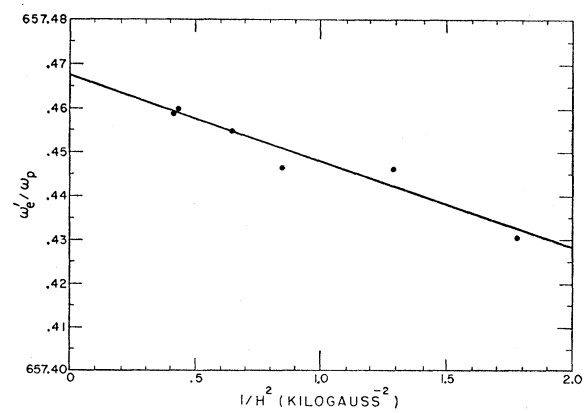

FIG. 8. Example of a typical run.

12. MAGNETIC MOMENT OF THE ELECTRON

We may obtain a value for the magnetic moment of the electron expressed in units of the Bohr magneton

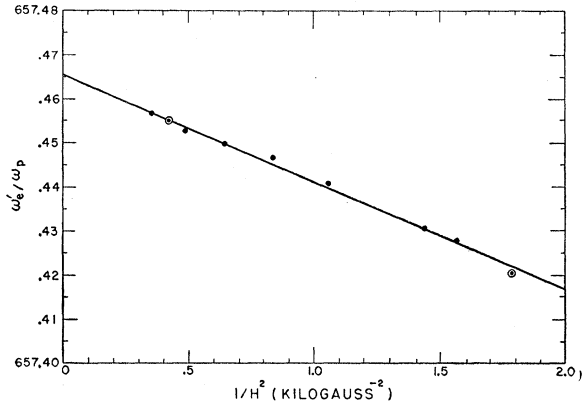

FIG. 9. Example of a good run. An encircled point indicates two separate determinations each yielding the same result.

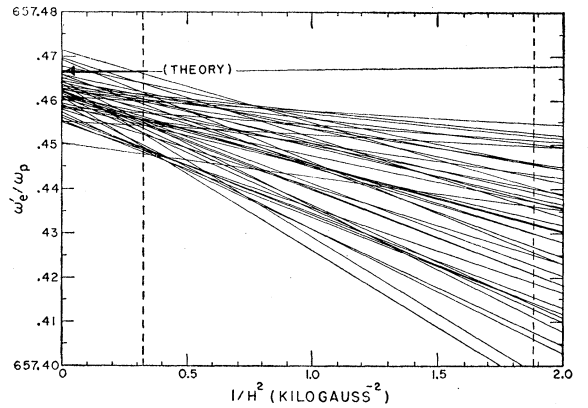

FIG. 10. Plots of the "straight lines" obtained for each of the forty-two runs. The slopes of the lines are those actually observed, but the lines have been vertically displaced to give the fully corrected intercept values that are presented for $\mu_0/\mu_{p(\text{oil})}$ in column (K) of Table III. The vertical dashed lines indicate the interval of magnetic field variation within which the data were taken. The heavy horizontal arrow at 657.467 indicates the terminal value of ω_e'/ω_p that should have been obtained for zero-energy electrons in order to yield the current theoretical estimate for the magnetic moment of the free electron $\mu_e/\mu_0=1.0011596$.

μ_e/μ_0 by combining our value for $\mu_{p(\text{oil})}/\mu_0$ with the experimentally determined value for $\mu_e/\mu_{p(\text{oil})}$.

Beringer and Heald[9] quote for the ratio of the magnetic moment of the free electron[29] to the magnetic

[29] Observations are actually performed upon hydrogenic electrons. Thus a relativistic correction must be applied in order to deduce the moment of the free electron. Because the fine structure constant $\alpha=e^2/\hbar c$ enters into the correction only quadratically, the

moment of the proton, the latter observed in a spherical sample of mineral oil,

$$\mu_0/\mu_{p(\text{oil})}=658.2298\pm0.0002. \quad (12.1)$$

We combine our value for $\mu_{p(\text{oil})}/\mu_0$, given in (11.1), with the result (12.1) to obtain for the magnetic moment of the free electron expressed in units of the Bohr magneton

$$\mu_e/\mu_0=1+(\alpha/2\pi)+(1.2\pm0.9)(\alpha^2/\pi^2)$$
$$=1.001168\pm0.000005(\cong 5 \text{ ppm}).$$
$$(50\% \text{ probable error}) \quad (12.2)$$

This result is to be compared with the current theoretical estimate[6,7] for the magnetic moment of the free electron:

$$\mu_e/\mu_0=1+(\alpha/2\pi)-0.328(\alpha^2/\pi^2)$$
$$=1.0011596. \quad (12.3)$$

We are not inclined to consider the discrepancy between

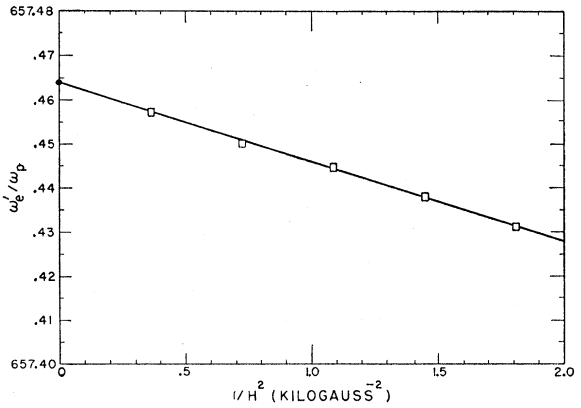

FIG. 11. Test of the "straight-line hypothesis." The points in this figure represent the averages of the results obtained, at the indicated values of magnetic field, for all runs.

the experimental result (12.2) and the theoretical result (12.3) to be significant.

13. MAGNETIC MOMENT OF THE FREE PROTON

We may obtain a value for the magnetic moment of the free proton, expressed in units of the Bohr magneton, by applying the diamagnetic correction factor appropriate for the mineral oil sample. Recalling that $\mu_{p(\text{oil})}/\mu_0=\omega_{p(\text{oil})}/\omega_e$, we may write

$$\frac{\mu_{p(\text{free})}}{\mu_0}=\frac{\mu_{p(\text{oil})}}{\mu_0}\left(\frac{\omega_p(H_2O)}{\omega_{p(\text{oil})}}\right)\times\left(\frac{\omega_p(H_2)}{\omega_p(H_2O)}\right)\left(\frac{\omega_{p(\text{free})}}{\omega_p(H_2)}\right)G, \quad (13.1)$$

where G is a bulk diamagnetic correction factor that involves the geometry of the sample. We have compared the proton signal from a 0.01-molal solution of $FeCl_3$ in distilled water with the signal from our sample of mineral oil (Squibb Heavy California Liquid Petrolatum) and found, for identically shaped (spherical) samples,

$$\omega_p(H_2O)/\omega_{p(\text{oil})}=1+(3.7\pm0.4)\times10^{-6}$$
$$(50\% \text{ probable error}). \quad (13.2)$$

Hardy[30] obtains identically this value when working with deoxygenated distilled H_2O; his uncertainty is $\pm0.1\times10^{-6}$. Because of the spherical nature of our sample, the generally small doping correction is actually zero. Hardy[30] quotes

$$\omega_p(H_2)/\omega_p(H_2O)=1-(0.6\pm0.1)\times10^{-6}, \quad (13.3)$$

for gaseous molecular hydrogen in comparison with the above mentioned water sample (both samples spherical). Ramsey[31] has calculated the magnetic shielding constant for molecular hydrogen and so has Newell[32]; their results are

$$\omega_{p(\text{free})}/\omega_p(H_2)=\begin{cases}1+(26.8)\times10^{-6}, & \text{(Ramsey)}\\ 1+(26.6\pm0.3)\times10^{-6}, & \text{(Newell).}\end{cases} \quad (13.4)$$

Because of the spherical form of all of the samples employed in the above measurements, the bulk diamagnetic correction factor G in (13.1) is equal to unity.

We combine the relations (13.2) and (13.3) with the average of the values given in (13.4) to obtain from (13.1)

$$\mu_{p(\text{free})}/\mu_0=(657.462\pm0.003)^{-1}\times[1+(3.7\pm0.4$$
$$-0.6\pm0.1+26.7\pm0.3)\times10^{-6}]$$
$$=(657.462\pm0.003)^{-1}\times[1+(29.8\pm0.5\times10^{-6}]$$
$$=(657.442\pm0.003)^{-1};$$
$$\mu_{p(\text{free})}=(1.521047\pm0.000007)\times10^{-3}$$
$$\text{Bohr magneton.} \quad (13.5)$$

The uncertainties indicated in the last two lines of (13.5) represent estimated 50% probable errors.

TABLE V. Estimated 50% probable errors in corrections applied to the raw data.

Source	Estimated 50% probable error (P_i)
(1) Variable magnetic corrections (see Sec. 10A)	±0.0025
(2) Relativistic correction (see Sec. 10B)	±0.0006
(3) Miscellaneous corrections (see Sec. 10C)	±0.0015

14. ACKNOWLEDGMENTS

The authors wish to thank their many colleagues at Stanford for valued discussions related to this experi-

recent 14.0 ppm modification of α (see the last reference in 3) does not significantly affect the quoted experimental value for the free electron moment.

[30] W. A. Hardy (private communication).
[31] N. F. Ramsey, Phys. Rev. **77**, 567 (1950); **78**, 699 (1950).
[32] G. F. Newell, Phys. Rev. **80**, 476 (1950).

ment, particularly Dr. Felix Bloch, Dr. Robert M. Cotts, Dr. Willis E. Lamb, Jr., Dr. George E. Pake, Dr. T. Michael Sanders, Dr. Richard M. Sands, and Dr. Lee R. Wilcox.

The authors wish to acknowledge the skillful assistance provided in the construction of various parts of the apparatus by Melvin B. Goodwin, Leonard L. Manning, and Burton G. Stuart of the Stanford University Physics Department shop. The authors also wish to express their thanks for the generous assistance provided by Mrs. Irene Ortenburger and Mr. James Anderson in the recording and processing of data.

One of the authors (S. L., Jr.) gratefully acknowledges the opportunity afforded him by the Department of Physics of Princeton University to fulfill his share of obligations related to the preparation of this report.

APPENDIX. QUANTUM MECHANICAL DERIVATION OF THE ELECTROSTATIC SHIFT

We wish to give a quantum mechanical derivation of Eq. (6.8). In the absence of any electric field, the Hamiltonian for an electron in a magnetic field is given by

$$\mathcal{H}_0=(1/2m)[\mathbf{p}+(e\mathbf{A}/c)]^2, \quad e>0. \tag{A1}$$

The energy eigenvalues W_n of the stationary states are equally spaced such that $W_n-W_{n-1}=\hbar\omega_e$; and the wave functions can be written[15]

$$\psi_n=f(y,z)H_n(x), \tag{A2}$$

where the $H_n(x)$ are harmonic oscillator wave functions. If an electrostatic field specified by the potential $\varphi(x,y)$[33] is introduced, the Hamiltonian for the system becomes modified by the addition to (A1) of a perturbation

$$\mathcal{H}'=-e\varphi(x,y). \tag{A3}$$

The resulting modification of the energy levels will give rise to shift $\Delta\omega$ in the frequency associated with the $(n, n-1)$ transition; we find from first order perturbation theory that

$$\Delta\omega=\frac{1}{\hbar}\left(\int\psi_n^*\mathcal{H}'\psi_n d\tau-\int\psi_{n-1}^*\mathcal{H}'\psi_{n-1}d\tau\right). \tag{A4}$$

[33] The explicit z dependence of φ is ignored here since it does not produce a first order shift in the cyclotron frequency.

The integrals appearing in (A4) may be evaluated by expanding $\mathcal{H}'$ in a Taylor series about the point (0,0):

$$\mathcal{H}'=-e\Big[\varphi_0+\left(\frac{\partial\varphi}{\partial x}\right)_0 x+\left(\frac{\partial\varphi}{\partial y}\right)_0 y+\tfrac{1}{2}\left(\frac{\partial^2\varphi}{\partial x^2}\right)_0 x^2 +\tfrac{1}{2}\left(\frac{\partial^2\varphi}{\partial y^2}\right)_0 y^2+\left(\frac{\partial^2\varphi}{\partial x\partial y}\right)_0 xy+\cdots\Big]. \tag{A5}$$

Those $\mathcal{H}'$ terms that contain an odd power of x will vanish upon integration of (A4). Furthermore, the unperturbed Hamiltonian $\mathcal{H}_0$ is invariant under rotation about the z axis so that for an arbitrary function $f(\xi)$,

$$\int\psi_n^* f(y)\psi_n d\tau=\int\psi_n^* f(x)\psi_n d\tau. \tag{A6}$$

Therefore,

$$\begin{aligned}&\int\psi_n^*\mathcal{H}'\psi_n d\tau\\ &=-e\left\{\varphi_0+\tfrac{1}{2}\left[\left(\frac{\partial^2\varphi}{\partial x^2}\right)_0+\left(\frac{\partial^2\varphi}{\partial y^2}\right)_0\right]\right\}\int\psi_n^* x^2\psi_n d\tau\\ &=-e\left\{\varphi_0+\tfrac{1}{2}\left[\left(\frac{\partial^2\varphi}{\partial x^2}\right)_0+\left(\frac{\partial^2\varphi}{\partial y^2}\right)_0\right]\right\}\frac{(2n+1)\hbar}{2m\omega_e},\end{aligned} \tag{A7}$$

where the expectation value for x^2 has been evaluated for the harmonic oscillator wave function.[17] We now obtain, by substituting (A7) into (A4)

$$\Delta\omega=-\frac{e}{2m\omega_e}\left[\left(\frac{\partial^2\varphi}{\partial x^2}\right)_0+\left(\frac{\partial^2\varphi}{\partial y^2}\right)_0\right]. \tag{A8}$$

Then, in terms of the electric field, the observed cyclotron frequency ω' is

$$\begin{aligned}\omega'&=\omega_e[1+(\Delta\omega/\omega_e)]\\ &=\omega_e\left\{1+\frac{mc^2}{2eH^2}\left[\left(\frac{\partial E_x}{\partial x}\right)_0+\left(\frac{\partial E_y}{\partial y}\right)_0\right]\right\},\end{aligned} \tag{A9}$$

where the field derivatives are evaluated at the orbit center. This expression is identical to Eq. (6.8).